FORECASTERS' FORUM

Mountain Wave Signatures in MODIS 6.7-μm Imagery and Their Relation to Pilot Reports of Turbulence

N. L. UHLENBROCK, K. M. BEDKA, W. F. FELTZ, AND S. A. ACKERMAN

Cooperative Institute for Meteorological Satellite Studies, University of Wisconsin—Madison, Madison, Wisconsin

(Manuscript received 15 June 2006, in final form 29 September 2006)

ABSTRACT

A technique for nowcasting turbulent mountain waves over the Front Range of the state of Colorado is investigated using Moderate Resolution Imaging Spectroradiometer (MODIS) water vapor (6.7 μm) channel imagery. Pilot reports of turbulence were examined to determine the probability of turbulence occurring when wave features were observed in the satellite imagery. Analysis of MODIS water vapor imagery indicated that mountain wave signatures were present for approximately 25% of the days during 2004. Approximately 75% of the severely turbulent days, as indicated by pilot reports, had wave signatures in the water vapor imagery. The wave signatures on the severely turbulent days had different characteristics in the imagery than the signatures on days that were less turbulent. The reports of severe turbulence were associated with complex patterns, the appearance of interference, or crossing wave fronts that extended downwind from the mountain ridge for a significant distance. The days that were less turbulent, as reported by pilots, had wave signatures with a simpler pattern, such as linear features orthogonal to the wind flow oriented parallel to one another.

1. Introduction

Turbulence is a hazard to both commercial and general aviation. A study of National Transportation Safety Board accident data for the years 1983–97 found that turbulence was responsible for 609 fatalities, 823 injuries, and an estimated loss of $134 million (Eichenbaum 2000). Hazardous turbulence can be grouped into two distinct categories: in cloud and clear air. In-cloud turbulence events are generally associated with strong vertical motions within the primary updraft of convective storms (Lane et al. 2003). Clear-air turbulence events are associated with a far more diverse set of atmospheric conditions: vertical wind shear near the upper-tropospheric jet stream (Endlich 1964), gravity waves along upper-tropospheric frontal zones (Koch et al. 2005) and above convective storms (Lane et al. 2003), and topographically induced (i.e., mountain) wave and rotor phenomena (Reiter and Foltz 1967; Clark and Gall 1982; Clark et al. 2000; Doyle and Durran 2002).

Mountain, or lee, waves are caused when air flows over mountain ridges within a stably stratified atmosphere (Durran 1986). Turbulence generated by mountain waves can be an aviation hazard due to strong vertical motions generated by these oscillating air currents. Clouds that form in the lee of mountain ranges are in rows quasi-parallel to the terrain disturbing the flow and orthogonal to the direction of the flow. In the absence of sufficient moisture in the atmosphere, wave clouds will not form, despite the fact that a well-developed lee wave may exist.

Satellite classification of orographic clouds began with the first weather satellite, the Television Infrared Operational Satellite (TIROS I), which was launched in 1960 (e.g., Conover 1964). Since then, mountain wave cloud signatures have been observed in satellite imagery in a number of studies (e.g., Fritz 1965; Ernst 1976; Ellrod 1986). This study makes use of the Moderate Resolution Imaging Spectroradiometer (MODIS; King et al. 1992; Salomonson et al. 2002) instruments aboard the National Aeronautics and Space Administration (NASA) Earth Observing System (EOS) *Aqua* and

Corresponding author address: Steven A. Ackerman, 1225 West Dayton St., Madison, WI 53706.
E-mail: stevea@ssec.wisc.edu

DOI: 10.1175/WAF1007.1

TABLE 1. Description of numerical PIREP scale, adapted from FAA AIM.

Turbulence	Description	Comments
0	None	
1	Smooth to light	
2	Light	Momentarily causes slight, erratic changes in altitude and/or attitude (pitch, roll, yaw); unsecured objects may be displaced slightly
3	Light to moderate	
4	Moderate	Changes in altitude or attitude occur but the aircraft remains in positive control at all times; occupants feel strain against seat belts; unsecured objects are dislodged
5	Moderate to severe	
6	Severe	Causes large abrupt changes in altitude and/or attitude, usually causing large variations in indicated airspeed and the aircraft becomes very hard to control; occupants are forced violently against seat belts; unsecured objects are tossed about
7	Severe to extreme	
8	Extreme	Aircraft is violently tossed about with control being virtually impossible and large sudden changes in altitude and/or attitude take place

Terra satellites. MODIS observations include measurements in the water vapor absorption channel at a 1-km nadir spatial resolution. These measurements provide a new opportunity to examine the spatial characteristics of mountain wave phenomena, particularly in clear-air conditions. The paper investigates mountain wave signatures in water vapor imagery as they relate to pilot reports of turbulence along the Colorado Front Range.

2. Observations

a. Pilot reports

Pilot reports (PIREPS) are statements issued by pilots to air traffic control facilities on the ground to alert them of potentially hazardous atmospheric conditions, ranging from low ceilings to convective weather (see Federal Aviation Administration 2006, chapter 7; hereafter FAA AIM). PIREPS are issued to the nearest ground facility with which communication is established, and that facility's location depends on the aircraft's current flight route location. The Enroute Flight Advisory Service (EFAS) is the central facility responsible for collecting and disseminating PIREPS to aircraft and air traffic control facilities. This service is specifically designed to provide weather and other dangerous condition briefings upon pilot request.

When pilots encounter turbulence and issue a PIREP, they are encouraged to include the following information: turbulence intensity, whether turbulence was in or near clouds, turbulence duration, aircraft type, location, and altitude. Aviation turbulence as reported in PIREPS is subjective as it is based on the response of the aircraft to the wind field rather than the turbulent state of the atmosphere. In an effort to mitigate the subjectivity, the FAA AIM includes a table with guidelines as to what constitutes light, moderate, severe, and extreme turbulence based on aircraft reaction and the reaction of passengers and objects inside the aircraft (see Table 1).

High-amplitude mountain waves, wind shear, rotors, and strong downslope windstorms can cause turbulence within and near mountainous regions. Relating PIREPs of turbulence caused by mountain waves at lower altitudes is complicated, since it is difficult to differentiate those reports from the turbulence caused by boundary layer processes. The mid- and high-altitude turbulence incidents are of particular interest to this study. The MODIS instruments on the *Aqua* satellite have overpasses of the Colorado region generally within 2 h of 0900 and 1900 UTC. PIREPS near the time of the 0900 UTC overpasses are generally scarce, as are flights during this time, so the analysis of MODIS data focused on imagery near 1900 UTC.

b. MODIS imagery

The Earth Observing System (EOS) is a group of NASA satellites whose observations of land surfaces, oceans, and the atmosphere are used to better understand the earth system and how it changes. Two of these EOS satellites are *Terra*, launched in 2000, and *Aqua*, launched in 2002. Both of these satellites are polar orbiting and carry the MODIS instruments (Salomonson et al. 2002). MODIS has 36 spectral bands for collecting information about the earth system. The solar bands have spatial resolutions of 250 m, 500 m, and 1 km, and the infrared bands have spatial resolutions of 1 km.

The MODIS instruments provide new ways in which to analyze atmospheric phenomena, including lee waves. MODIS channel 27 (6.535–6.895 μm) provides upper-tropospheric water vapor imagery at 1-km spatial resolution. Radiation at these wavelengths measured by the satellite sensor represents energy emitted

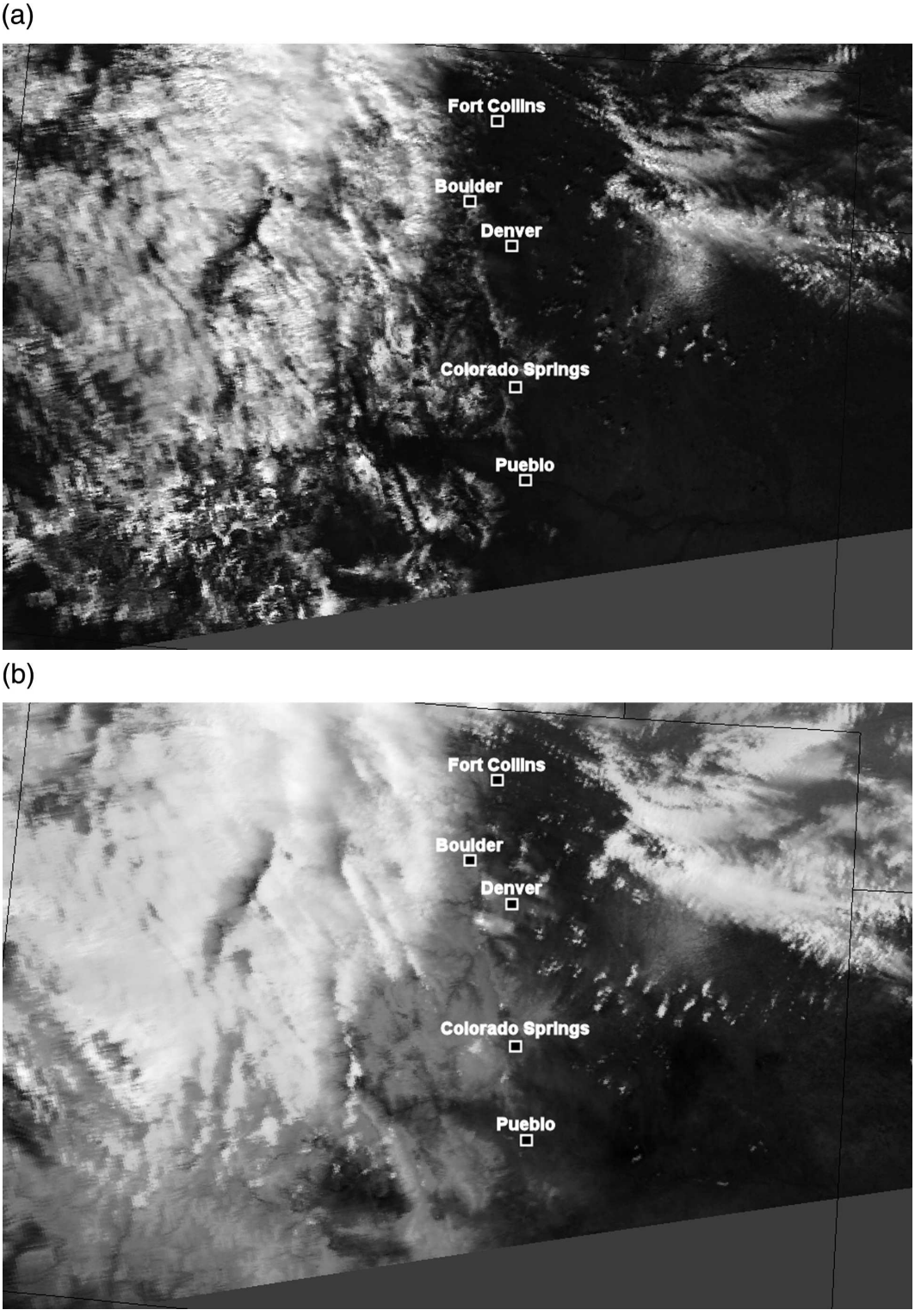

FIG. 1. (a) MODIS visible, (b) destriped infrared window, and (c) destriped water vapor imagery from 6 Mar 2004, indicating the utility of the 6.7-μm water vapor channel for the detection of atmospheric mountain wave features.

(c)

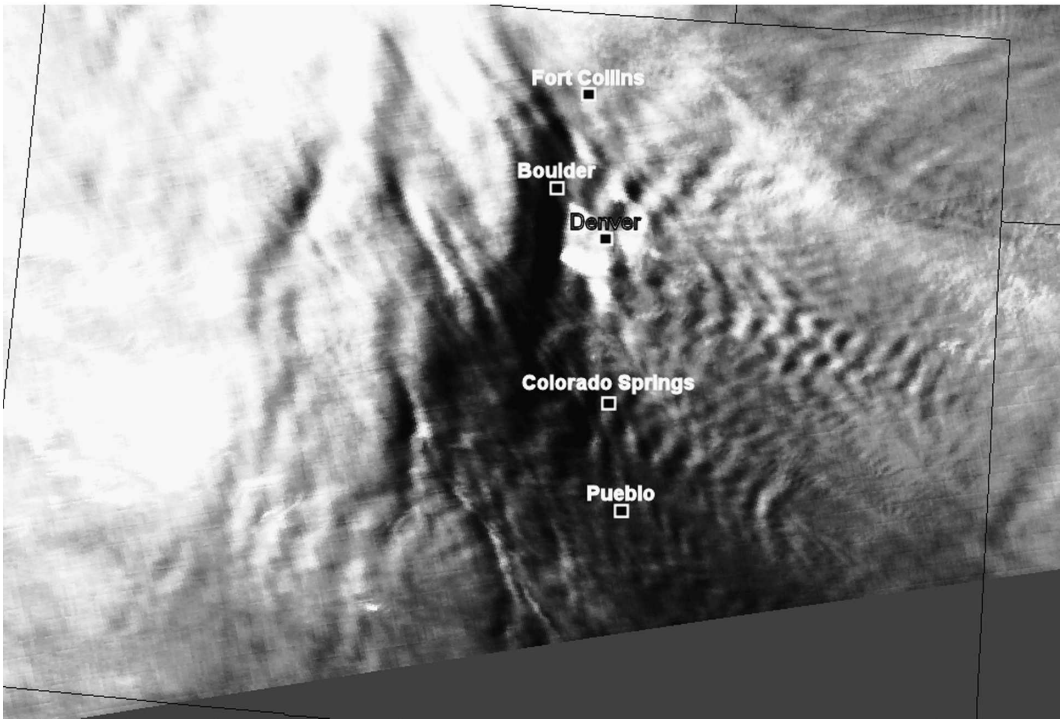

FIG. 1. (*Continued*)

by water vapor in the middle and upper troposphere, providing forecasters with useful information on the flow patterns at these levels. While the water vapor channel can occasionally observe the surface (Ackerman et al. 2005), most of the radiant energy observed by the satellite is coming from altitudes above approximately 550 hPa (or 15 000 ft in a standard atmosphere). Typically, observations from geostationary satellites at this wavelength are used to provide information on large-scale flow. The 1-km resolution of MODIS reveals the presence of lee waves in both clear and cloudy skies. Figure 1 demonstrates the utility of the MODIS water vapor imagery by presenting visible, infrared window, and water vapor imagery for 6 March 2004. The mountain wave features are nonexistent or subtle within the visible and infrared window but very apparent in the 6.7-μm-channel water vapor imagery. This study uses these MODIS water vapor observations to characterize lee waves as a function of PIREP indications of turbulence.

The MODIS 1-km images are composed of measurements from 10 detectors. Variability in the calibration of the detectors leads to "striping" in the imagery. To minimize these detector-to-detector artifacts, the MODIS bands have been destriped with an algorithm developed at the Space Science and Engineering Center (SSEC) at the University of Wisconsin—Madison [C. Moeller and L. Gumley (2006), personal communication, based on the work of Weinreb et al. (1989)].

MODIS imagery over the Front Range region of Colorado was monitored for mountain wave signatures for every day during the year 2004. Eighty-nine days exhibited lee-wave features in the water vapor channel. This 1-yr study is designed to determine the presence or absence of lee waves in the imagery, but does not provide direct information on the severity or longevity of the events. Turbulence associated with a lee-wave pattern is assessed using pilot reports of turbulence, which are subjective in nature. The MODIS imagery is used only to categorize the appearance of the waves. Our approach was to determine if the severity of lee-wave turbulence, as defined by PIREP, could be categorized based on the wave pattern observed by the satellite image.

Lee waves are capable of causing turbulence at all levels of intensity (Clark et al. 2000), but not all lee waves cause turbulence. The focus for this study is the turbulence reports deemed moderate or greater: a number of four or higher in the pilot reports. An average number per day of moderate or greater reports within Colorado was calculated for the year 2004, as well as the standard deviation. To determine how tur-

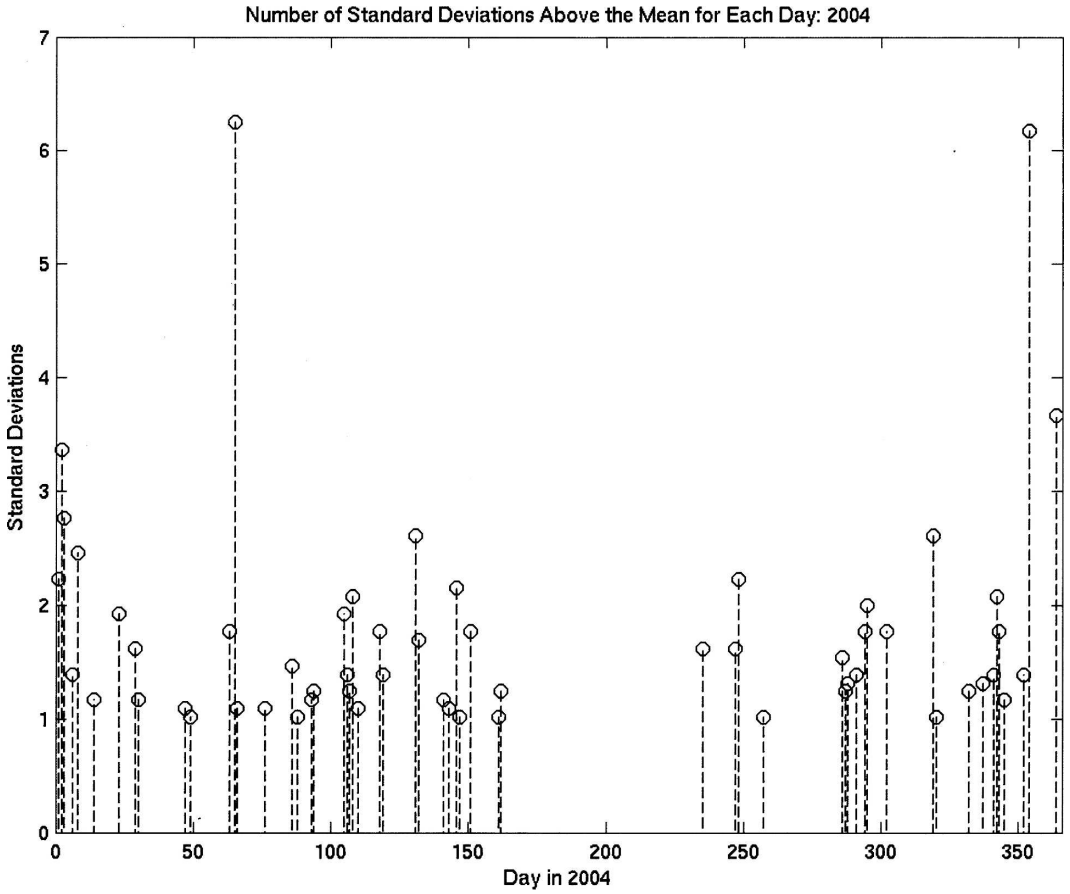

FIG. 2. Number of std devs above the mean number of moderate or greater turbulence reports in 2004 by day.

bulent each day in 2004 was in relation to the normal value for the year, the average daily value in 2004 was subtracted from the daily number of reports for each day. If the result was positive, it was then divided by the standard deviation (1 std dev = 13.17).

Figure 2 shows a plot of the number of standard deviations beyond the average daily value in 2004. For the entire 1-yr study period, there were 1776 turbulent PIREPS found within the state of Colorado, corresponding to a mean of roughly five turbulence reports

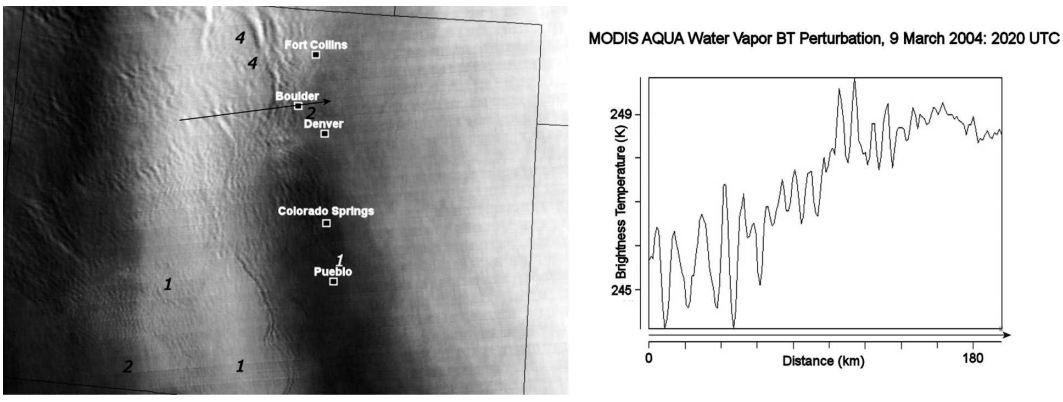

FIG. 3. (left) Destriped *Aqua* MODIS water vapor image at 2020 UTC 9 Mar 2004 representing pattern 1. Plotted numbers represent the turbulence intensity at the PIREP locations within ±2 h of the MODIS image. (right) The 6.7-μm brightness temperature image across the transect marked in the image to the left.

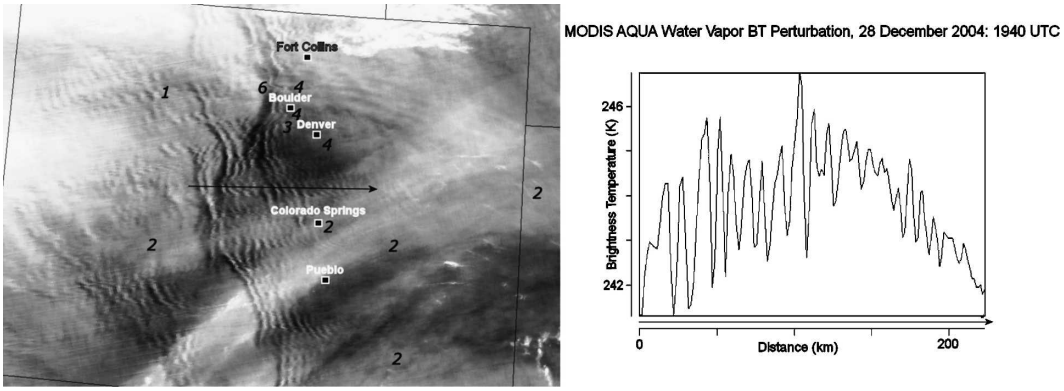

FIG. 4. As in Fig. 3 but for image at 1940 UTC 28 Dec 2004 representing pattern 2.

per day. Fifty-six days had a number of moderate or greater turbulence reports that exceeded the mean by at least one standard deviation. Of these 56 days, 26, or about 46%, exhibited wave signatures in the MODIS imagery. Thirteen days exceeded the mean by at least two standard deviations, and 9 of those 13 days (or about 70%) exhibited wave signatures in the satellite water vapor imagery. There are two days that had a significantly higher number of turbulence reports in Colorado and had wave signatures; 6 March and 20 December each exceeded the mean number of turbulence reports by over six standard deviations.

3. Lee-wave patterns in MODIS imagery

The wave signatures from the satellite imagery were examined for pattern differences between turbulent days and those on less turbulent days. Lee waves were grouped into one of six main patterns based on their appearance in the MODIS water vapor imagery in the Front Range region of northern Colorado. The six main patterns are as follows, and the associated figures are examples of each type.

Pattern 1 includes imagery in which the brightness temperature gradient across the waves is small (low amplitude) and the downstream extent of the pattern is small. The *Aqua* MODIS water vapor image at 2020 UTC 9 March 2004 is an example of this type of category 1 case (Fig. 3). In addition to the 6.7-μm brightness temperature image, Fig. 3 also shows the 6.7-μm brightness temperature ($BT_{6.7}$) across the transect marked in the image to the left. The $BT_{6.7}$ variations across the wave pattern are generally less then 3 K.

Pattern 2 includes images that appear to have a low-amplitude wave that extends downstream from the mountain ridge, as was the case at 1940 UTC 28 December 2004 (Fig. 4). The $BT_{6.7}$ variations across the wave pattern are generally less then 3 K, but the waves extend approximately 100 km out into the Great Plains.

Pattern 3 imagery is similar to category 2 except that the wave structure appears to include an interference pattern. An example case is shown for 2040 UTC 14

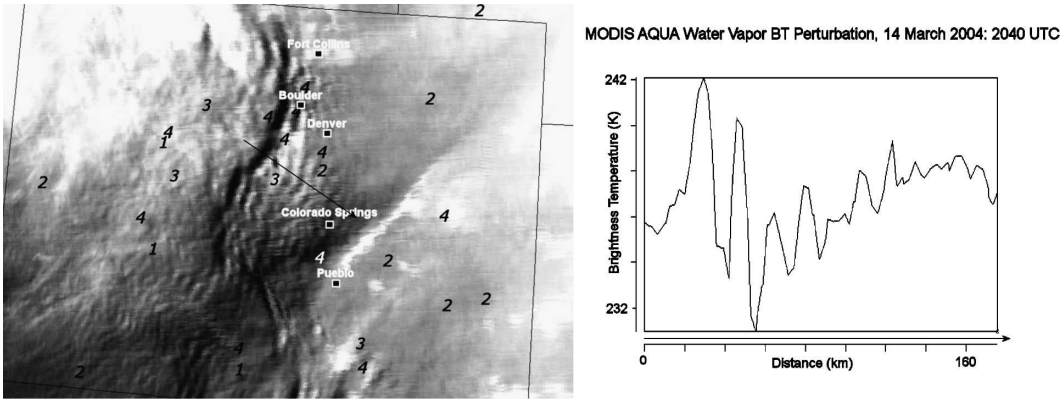

FIG. 5. As in Fig. 3 but for image at 2040 UTC 14 Mar 2004 representing pattern 3.

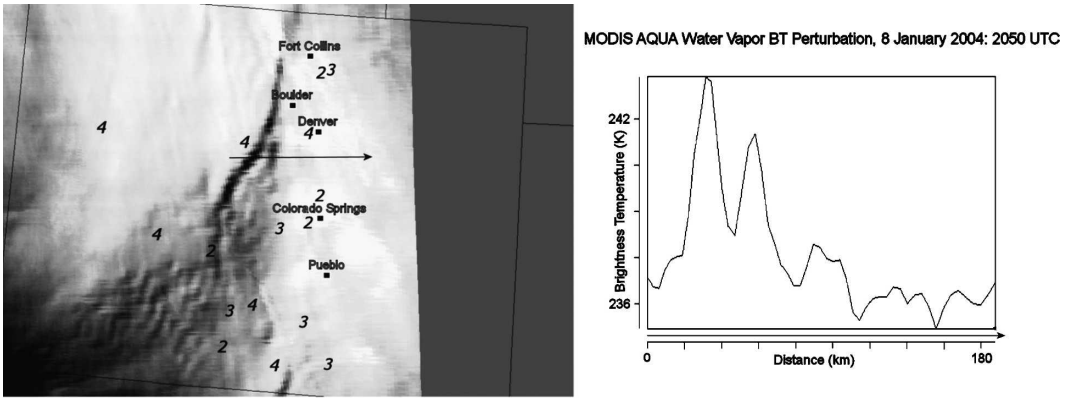

FIG. 6. As in Fig. 3 but for image at 2050 UTC 8 Jan 2004 representing pattern 4.

March 2004 (Fig. 5). The $BT_{6.7}$ variations are generally less then 4 K in this case, but the waves extend out into the Great Plains and appear to have a herringbone-type structure, indicating some degree of wave interference.

Pattern 4 imagery includes waves that have a large $BT_{6.7}$ gradient around the northern Front Range, but have a short extent downstream. An example case occurred at 2050 UTC 8 January 2004 (Fig. 6). The $BT_{6.7}$ gradient across the primary wave is 6 K but it is closely anchored to the mountain range and does not extend into the Great Plains.

Pattern 5 includes what appear to be high-amplitude waves that extend downstream, though there is little or no interference pattern in the imagery. The *Aqua* MODIS water vapor image at 2010 UTC 3 September 2004 represents category 5 (Fig. 7). The wave patterns extend out to the Great Plains and in the vicinity of the Front Range, the $BT_{6.7}$ gradient is generally greater then 4 K, and the wavelength is about 12 km.

Pattern 6 images are similar to those of pattern 5, except that the wave pattern exhibits interference. An example is the case at 1950 UTC 6 March 2004 (Fig. 8). On this day, the $BT_{6.7}$ gradient is greater then 5 K near the Front Range and extends into the Great Plains with a herringbone-type interference pattern. The waves occur over 200 km downwind from the mountains with a wavelength of approximately 15 km.

Table 2 shows the number of incidences of each pattern and the number of days for that pattern in which the turbulence reports exceeded the mean by at least one standard deviation for each pattern. After categorizing the 89 wave events (see Table 1), the two most common types were low amplitude with short downstream extent (pattern 1), and low amplitude with long downstream extent, little or no interference, and short wavelengths (pattern 2). The two least common types were low amplitude with long downstream extent, high amounts of interference, and long wavelengths; and high amplitude with long downstream extent, high amounts of interference, and short wavelengths. Patterns 3, 4, and 6 were the most likely to be associated with pilot-reported turbulence. Both patterns 3 and 6 contain a herringbone-type interference pattern. The pattern in the water vapor imagery appears to arise

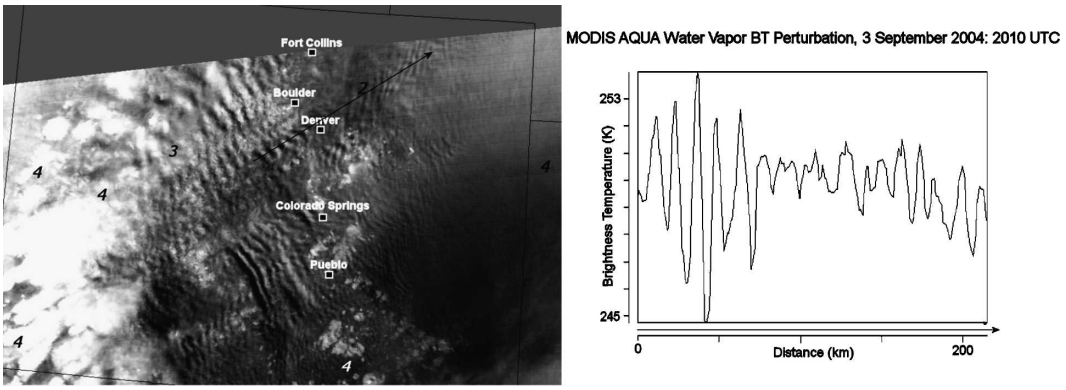

FIG. 7. As in Fig. 3 but for image at 2010 UTC 3 Sep 2004 representing pattern 5.

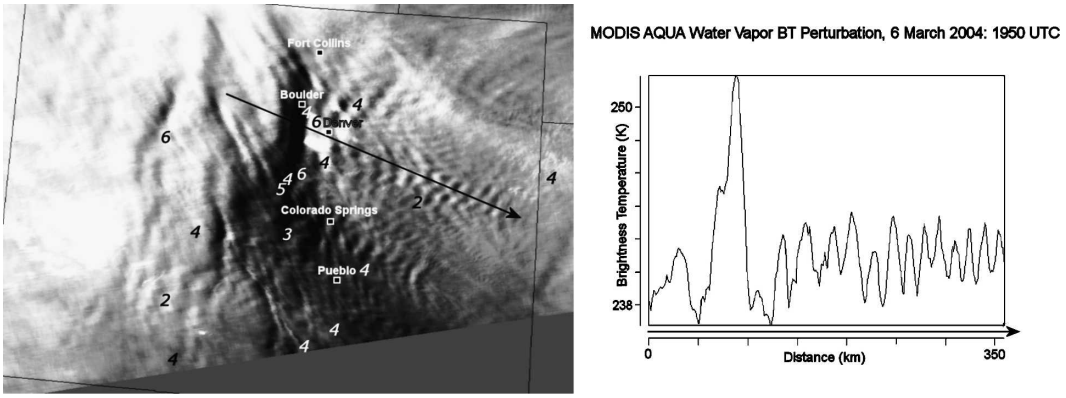

FIG. 8. As in Fig. 3 but for image at 1950 UTC 6 Mar 2004 representing pattern 6.

form two waves coming from different directions, interacting, and generating this interference type pattern.

4. Summary

The combined analysis of pilot reports (PIREPS) of turbulence and MODIS imagery over the Colorado Front Range region during 2004 indicates that the higher the daily number of reports was above the yearly mean, the more likely it was that lee waves were seen in the satellite imagery. The presence of mountain wave signatures in the imagery did not necessarily signify a day with a high frequency of turbulent events of moderate intensity or higher. Thus, while a day with many PIREP reports of moderate intensity almost certainly exhibited mountain wave signatures, a day that exhibited mountain wave signatures in the satellite imagery could not always be considered extremely turbulent.

The satellite image analysis of the wave patterns, in conjunction with the turbulence severity noted by the PIREPS, indicated that waves exhibiting interference were concurrent with reports of high amounts of turbulence. This is supported by the fact that 13 of the 22 cases with interference were associated with many PIREP reports of turbulence, while only 16 of the 67 cases without interference were classified as turbulent. These numbers suggest that the interference pattern is associated with a high frequency of reported turbulence. While the results suggest that turbulence (intensity and the number of reports) cannot be determined with high probability from the pattern of the imagery alone, the study presents first results that can be used as a starting point for interpreting the probability of turbulence based on the observation of wave patterns. Combining the satellite water vapor imagery with wind measurements, from a wind profiler or radiosonde, along with information on thermal stability above the mountain barrier might provide a better nowcast of turbulence than do the wave patterns alone.

TABLE 2. The number of times a given pattern occurred in the MODIS imagery for the 1-yr study period. Also, the number of days that the PIREP turbulence reports exceeded the mean number of reports by at least one std dev.

Pattern	No. of wave events	No. of turbulent days
1	18	2
2	27	5
3	15	7
4	9	5
5	13	4
6	7	6

The MODIS instruments typically view one location of the middle latitudes three to four times in a 24-h period at high spatial resolution. The current Geostationary Operational Environmental Satellites (GOES) make a complete image over the continental United States once every 15 min during normal operation, at 4-km resolution in the infrared, which is a bit too coarse to highlight the detailed interference patterns shown by MODIS. The next-generation GOES satellites will improve our capability to monitor the weather and atmospheric conditions. The Advanced Baseline Imager (ABI) instrument on the GOES-R satellite, scheduled for launch in 2012, will have 16 spectral bands, a 5-min scan time for the continental United States, and 2-km resolution for infrared bands, including the water vapor channel (Schmit et al. 2005). The ABI instrument will improve our ability to monitor the formation and dissipation of these mountain wave signatures.

Acknowledgments. This work was supported by the NASA Applied Sciences Program and the NASA Aviation Safety and Security Program through the NASA Advanced Satellite Aviation Weather Products

(ASAP) project (Grant 4400071484). Addition support was provided by NOAA Grant NA07EC0676. The authors thank Mr. John Murray, NASA Langley Research Center; Dr. Robert Sharman, NCAR; and Mr. Tim Schmit (NOAA/NESDIS) for their enthusiastic support of this work. We would also like to acknowledge Tom Rink and Tom Whittaker for their extensive Integrated Data Viewer visualization support.

REFERENCES

Ackerman, S. A., S. Bachmeier, K. Strabala, and M. Gunshor, 2005: A satellite view of the cold air outbreak of 13–14 January 2004. *Wea. Forecasting,* **20,** 222–225.

Clark, T. L., and R. Gall, 1982: Three-dimensional numerical model simulations of airflow over mountainous terrain: A comparison with observations. *Mon. Wea. Rev.,* **110,** 766–791.

——, W. D. Hall, R. M. Kerr, D. Middleton, L. Radke, F. M. Ralph, P. J. Neiman, and D. Levinson, 2000: Origins of aircraft-damaging clear-air turbulence during the 9 December 1992 Colorado downslope windstorm: Numerical simulations and comparison with observations. *J. Atmos. Sci.,* **57,** 1105–1131.

Conover, J. H., 1964: The identification and significance of orographically induced clouds observed by TIROS satellites. *J. Appl. Meteor.,* **3,** 226–234.

Doyle, J. D., and D. R. Durran, 2002: The dynamics of mountain-wave-induced rotors. *J. Atmos. Sci.,* **59,** 186–201.

Durran, D. R., 1986: Mountain waves. *Mesoscale Meteorology and Forecasting,* P. S. Ray, Ed., Amer. Meteor. Soc., 472–492.

Eichenbaum, H., 2000: Historical overview of turbulence accidents. Rep. TR-7100/023-1, MCR Federal, Inc., 59 pp.

Ellrod, G., 1986: Uses of satellite imagery in turbulence detection. *Proc. 24th Aerospace Sciences Meeting,* Reno, NV, American Institute of Aeronautics and Astronautics, 258–265.

Endlich, R. M., 1964: The mesoscale structure of some regions of clear-air turbulence. *J. Appl. Meteor.,* **3,** 261–276.

Ernst, J. A., 1976: SMS-1 nighttime infrared imagery of low-level mountain waves. *Mon. Wea. Rev.,* **104,** 207–209.

Federal Aviation Administration, cited 2006: Aeronautical Information Manual. [Available online at http://www.faa.gov/airports_airtraffic/air_traffic/publications/atpubs/aim/.]

Fritz, S., 1965: The significance of mountain lee waves as seen from satellite pictures. *J. Appl. Meteor.,* **4,** 31–37.

King, M. D., Y. J. Kaufman, W. P. Menzel, and D. Tanré, 1992: Remote sensing of cloud, aerosol, and water vapor properties from the Moderate Resolution Imaging Spectrometer (MODIS). *IEEE Trans. Geosci. Remote Sens.,* **30,** 2–27.

Koch, S. E., and Coauthors, 2005: Turbulence and gravity waves within an upper-level front. *J. Atmos. Sci.,* **62,** 3885–3908.

Lane, T. P., R. D. Sharman, T. L. Clark, and H.-M. Hsu, 2003: An investigation of turbulence generation mechanisms above deep convection. *J. Atmos. Sci.,* **60,** 1297–1321.

Reiter, E. R., and H. P. Foltz, 1967: The prediction of clear air turbulence over mountainous terrain. *J. Appl. Meteor.,* **6,** 549–556.

Salomonson, V., W. L. Barnes, X. Xiong, S. Kempler, and E. Masuoka, 2002: An Overview of the Earth Observing System MODIS Instrument and associated data systems performance. *Proc. Int. Geoscience and Remote Sensing Symp.,* Sydney, Australia, IEEE/GRSS, 1174–1176.

Schmit, T. J., M. M. Gunshor, W. P. Menzel, J. J. Gurka, J. Li, and S. Bachmeier, 2005: Introducing the next-generation Advanced Baseline Imager (ABI) on GOES-R. *Bull. Amer. Meteor. Soc.,* **86,** 1079–1096.

Weinreb, M. P., R. R. Xie, J. H. Lienesch, and D. S. Crosby, 1989: Destriping GOES images by matching empirical distribution functions. *Remote Sens. Environ.,* **29,** 185–195.